

Adsorption of critical and supercritical fluids

S. B. Kiselev^{a)} and J. F. Ely

Chemical Engineering and Petroleum Refining Department, Colorado School of Mines, Golden, Colorado 80401-1887

M. Yu. Belyakov

Institute for Oil and Gas Research of the Russian Academy of Sciences, Leninsky Prospect 63/2, Moscow 117917, Russia

(Received 10 August 1999; accepted 10 November 1999)

We develop a crossover theory for critical adsorption of pure fluids in a semi-infinite system. In our previous publication [Phys. Lett. A **251**, 212 (1999)] we applied the theory to the analysis of experimental data for adsorption of liquid SF₆ on the critical isochore only. In this article we extend the theory on the noncritical isochores and present a comparison of the theoretical predictions for the surface excess (Gibbs) adsorption with experimental data for CO₂/silica and SF₆/graphite systems. Good representation of experimental data is achieved in the range of temperatures from the saturated temperature up to 1.15 T_c and densities $0.5\rho_c \leq \rho \leq 1.5\rho_c$. The optimization of the model to the excess isotherms in both systems indicates that they have surface critical behavior in the universality class of *normal* transition. However, in this case model does not reproduce the excess adsorption data for SF₆/graphite system at temperatures $\tau = T/T_c - 1 \leq 0.02$ at $\rho = \rho_c$. Analysis of the excess adsorption data along the critical isochore in SF₆/graphite system indicates that the surface field h_1 vanishes linearly with τ as $T \rightarrow T_c$, which corresponds to the *ordinary* transition. © 2000 American Institute of Physics. [S0021-9606(00)50406-1]

I. INTRODUCTION

A characteristic feature of critical phenomena in fluids is the presence of long-range fluctuations in the density. The intensity of these fluctuations diverges as the critical point is approached. As a consequence, the thermodynamic surface of a fluid exhibits a singularity at the critical point which can be described in terms of the universal scaling laws with universal exponents and universal scaled functions.^{1,2} The physical adsorption of fluids under critical and supercritical conditions onto solid surfaces also exhibits the effects of long-range density fluctuations. The surface excess, or Gibbs, adsorption of pure fluids on the surface is defined as

$$\Gamma = \int_0^\infty (\rho(z) - \rho) dz, \quad (1)$$

where $\rho(z)$ is the density of fluid at a distance z from the surface, and $\rho = \rho(\infty)$ is the bulk density of the fluid. When a fluid bounded by a surface approaches its critical point, at $\rho = \rho_c$ and reduced temperatures $|\tau| = |T/T_c - 1| \ll Gi$ (T_c is the critical temperature and Gi is the Ginzburg number) the adsorption Γ exhibits singular behavior,³ just as the bulk properties.^{1,2} This phenomenon is known as critical adsorption. The classical theories of adsorption, such as the Langmuir and BET theories,⁴ and the recently developed local density model⁵⁻⁷ give a reasonable representation of the adsorption data far away from the critical point. However, all these analytical theories fail to reproduce the nonanalytical singular behavior of the adsorption in the vicinity of the bulk

critical point. The local density model,⁵⁻⁷ for example, based on the empirical Peng–Robinson equation of state, contains mean-field values of the asymptotic critical exponents. Just as the Peng–Robinson equation of state gives a singularity for the isobaric heat capacity, the local density model⁵⁻⁷ also yields a singularity for the excess adsorption in the asymptotic critical region, but with wrong critical exponent. Therefore, this engineering model cannot be applied to the analysis of critical adsorption data in the vicinity of the bulk critical point. The more rigorous integral equation approaches^{8,9} also fail in the critical region, because the equations cannot be closed.

In order to reproduce the nonanalytical singular behavior of the adsorption in the critical region, the scaled expressions for the density $\rho(z)$, or more generally for the order-parameter profile $m(z)$, in Eq. (1) should be used. The scaling hypothesis for the order-parameter in semiinfinite systems was first formulated by Fisher and de Gennes.³ According to their hypothesis, the order-parameter profile $m(z)$ near a surface for a system in zero external field $h = 0$ can be represented in the universal form

$$m(z) = m_0 \tau^\beta P_\pm(\zeta), \quad (2)$$

where $\zeta = z/\xi_b \geq 0$ is the dimensionless distance from the surface, $\xi_b = \xi_0 \tau^{-\nu}$ is the correlation length in the bulk fluid, m_0 and ξ_0 are the system-dependent critical amplitudes, and $\beta = 0.325$ and $\nu = 0.625$ are universal critical exponents. In the disordered phase [$T > T_c$, $m_b = m(\infty) = 0$], the scaled function has the asymptotes

$$P_+^{\text{FdG}}(\zeta) = \begin{cases} P_0 \zeta^{-\beta/\nu}, & \text{for } \zeta \ll 1, \\ P_\infty e^{-\zeta}, & \text{for } \zeta \gg 1, \end{cases} \quad (3)$$

^{a)} Author to whom all correspondence should be addressed. Electronic mail: skiselev@mines.edu

where P_0 and P_∞ are universal constants.

During the last two decades the bulk properties of the system near the second-order phase transition, including the crossover from critical scaling to analytical classical behavior, have been studied in detail.^{10–14} During the same time the theory of boundary critical phenomena has focused only on the study of the asymptotic critical region (for a review, see Ref. 15). Theoretical expressions for the scaling function $P_\pm(\xi)$ (Refs. 16–19) have been obtained to first order in ϵ ($\epsilon=4-d$, where d is the dimensionality), give incorrect values of the critical exponents, and do not crossover into the classical mean-field equations when $Gi \ll |\tau| \ll 1$. All these expressions have been obtained only for the zero external field $h=0$ ($\rho=\rho_c$ for pure fluids), and cannot be extrapolated to the entire critical region.

For zero external field, the crossover expressions for the order-parameter profile and the critical adsorption obtained to first order in ϵ and their phenomenological generalizations have been discussed in detail in our previous publications.^{20,21} In this work, we develop a crossover expression for the order-parameter profile in nonzero external field and apply this expression to the analysis of the surface excess adsorption data of supercritical CO₂ on the octadecyl-bonded silica^{22,23} and of near-critical SF₆ on a graphite substrate.²⁴

In Sec. II we review the mean-field theory results for the critical adsorption. The crossover expression for the order-parameter profile is described in Sec. III. A comparison of the crossover model with the surface excess adsorption data is presented in Sec. IV, and we discuss the results in Sec. V.

II. MEAN-FIELD THEORY

The mean-field (MF) approach to critical phenomena in semiinfinite systems in zero external field has been studied by many authors and its results are well-known.^{25–27} Therefore, here we give only a brief description of the MF approach and derive the mean-field expressions for the order-parameter profile, surface order parameter, and adsorption in the arbitrary nonzero external field.

A. Order-parameter profile

A field-theoretical description for the critical adsorption starts from the Landau–Ginzburg–Wilson effective Hamiltonian for the scalar order parameter $m=m(z)$ in a semiinfinite system^{26,25}

$$H = \frac{1}{V} \int d\vec{x}_\parallel \int_0^\infty dz (a_0 m^2 + u_0 m^4 + c_0 (\nabla m)^2 - hm), \quad (4)$$

where V is the total volume of the system, \vec{x}_\parallel is $(d-1)$ -dimensional vector parallel to the wall at $z=0$, h is the external ordering field, $a_0=\alpha_0\tau$, and $\alpha_0, u_0, c_0 > 0$ are the system-dependent coefficients.

Using translational invariance parallel to the surface, the mean-field order-parameter profile $m(z)$ is found from the equation

$$\frac{\delta H}{\delta m} = 0, \quad (5)$$

which for the effective Hamiltonian as given by Eq. (4) is equivalent to the Euler–Lagrange equation

$$2c_0 \left(\frac{d^2 m}{dz^2} \right) = 2\alpha_0 \tau m + 4u_0 m^3 - h, \quad (6)$$

with the boundary conditions:

$$m(z=0) = m_1, \quad m(z \rightarrow \infty) = m_b, \quad (7)$$

$$\left(\frac{d^2 m}{dz^2} \right)_{z \rightarrow \infty} = \left(\frac{dm}{dz} \right)_{z \rightarrow \infty} = 0.$$

The equation of state for the bulk fluid, with the bulk order-parameter m_b , in this case has the form

$$h = 2\alpha_0 \tau m_b + 4u_0 m_b^3. \quad (8)$$

The first integral of Eq. (6) can be written as

$$c_0 \left(\frac{dm}{dz} \right)^2 = \alpha_0 \tau (m^2 - m_b^2) + u_0 (m^4 - m_b^4) - h(m - m_b). \quad (9)$$

Using Eq. (8), it is easy to show that

$$\alpha_0 \tau (m^2 - m_b^2) + u_0 (m^4 - m_b^4) - h(m - m_b) = u_0 (m - m_b)^2 \left[m^2 + 2m_b m + \frac{\alpha_0 \tau + 3u_0 m_b^2}{u_0} \right], \quad (10)$$

and, after integration of Eq. (9), we obtain for the order-parameter profile in the MF approximation

$$m(z) = m_b \pm \frac{2\sqrt{\kappa} \exp(\bar{z} + \bar{z}_0)}{(\exp(\bar{z} + \bar{z}_0) \mp 2m_b / \sqrt{\kappa})^2 - 1}, \quad (11)$$

where the top signs (“+” and “−”) correspond to the decreasing order-parameter profile ($m_1 \geq m \geq m_b$) and the bottom signs (“−” and “+”) to the increasing order-parameter profile ($m_1 \leq m \leq m_b$), respectively. The parameter

$$\bar{\kappa} = (\alpha_0 \tau + 6u_0 m_b^2) / u_0 = 2\bar{m}_0^2 \tau + 6m_b^2 = 2\bar{M}^2 + 6m_b^2, \quad (12)$$

where $\bar{M} = \bar{m}_0 \tau^{1/2}$, and $\bar{m}_0 = \sqrt{\alpha_0 / 2u_0}$ is the amplitude of the bulk order parameter on the coexistence curve in the mean-field approximation [see Eq. (8) at $h=0$ and $\tau < 0$]

$$\bar{m}_{cxs} = \pm \bar{m}_0 |\tau|^{1/2} \quad \text{at } T \leq T_c. \quad (13)$$

The dimensionless distances \bar{z} and \bar{z}_0 in Eq. (11) are given by

$$\bar{z} = \frac{z}{\xi_b}, \quad \bar{z}_0 = \frac{z_0}{\xi_b} = \ln \left[\frac{1}{|\Delta m_1|} \left(\sqrt{\bar{\kappa}} + 2 \frac{m_b}{\sqrt{\bar{\kappa}}} \Delta m_1 + \sqrt{\Delta m_1^2 + 4m_b \Delta m_1 + \bar{\kappa}} \right) \right], \quad (14)$$

where $\Delta m_1 = m_1 - m_b$, and $\xi_b = \sqrt{c_0 / u_0 \bar{\kappa}} = \xi_0 \sqrt{2\bar{m}_0^2 / \bar{\kappa}}$ is the bulk correlation length in MF approximation. The bulk order parameter m_b is determined, at fixed τ and h , from the equation of state as given by Eq. (8). For the zero external

field ($h=0$ at $\tau \geq 0$) $m_b=0$, and Eq. (11) is transformed into the well-known MF expression for the order-parameter profile in the semi-infinite system¹⁶

$$m(z) = \pm \frac{\bar{M}\sqrt{2}}{\sinh(\bar{z} + \bar{z}_0)}, \quad (15)$$

where dimensionless distances \bar{z} and \bar{z}_0 are

$$\bar{z} = z\tau^{1/2}/\bar{\xi}_0, \quad \bar{z}_0 = \ln\left(\sqrt{1 + 2\left(\frac{\bar{M}}{m_1}\right)^2} + \sqrt{2}\frac{\bar{M}}{m_1}\right), \quad (16)$$

and $\bar{\xi}_0 = \sqrt{c_0/\alpha_0}$ is the amplitude of the bulk correlation length in the zero external field (at $h=0$ and $\tau > 0$) $\bar{\xi}_b = \bar{\xi}_0\tau^{-1/2}$ in the mean-field approximation. In the case of the infinite adsorption, $m_1 \rightarrow \infty$, Eq. (15) can be rewritten in the universal form

$$m(z) = \bar{m}_0\tau^{1/2}\bar{P}_+(\bar{z}), \quad (17)$$

where $\bar{P}_+(\bar{z}) = \sqrt{2}/\sinh(\bar{z})$ is a MF prototype of the scaling function $P_+(\zeta)$.

The adsorption is given by

$$\Gamma = \int_0^\infty (m(z) - m(\infty))dz = \int_{m_1}^{m_b} (m - m_b)\left(\frac{dm}{dz}\right)^{-1} dm, \quad (18)$$

which after substitution of Eq. (15) and integration can be written in the form

$$\Gamma = \frac{\bar{\xi}_0\bar{m}_0}{\sqrt{2}} \ln\left[\frac{m_1 + m_b + \sqrt{m_1^2 + 2m_b m_1 - 3m_b^2 + \bar{\kappa}}}{2m_b + \sqrt{\bar{\kappa}}}\right]^2, \quad (19)$$

which coincides with corresponding expression obtained earlier by Marconi.²⁸

In the zero external field $h=0$ ($m_b=0$ at $\tau \geq 0$), Eq. (19) is transformed into

$$\begin{aligned} \Gamma &= \frac{\bar{\xi}_0\bar{m}_0}{\sqrt{2}} \ln\left(\frac{m_1}{\tau\bar{m}_0} \sqrt{2\tau + \left(\frac{m_1}{\bar{m}_0}\right)^2} + \frac{m_1^2}{\tau\bar{m}_0^2} + 1\right) \\ &= \frac{\bar{\xi}_0\bar{m}_0}{\sqrt{2}} \ln\left(\frac{m_1}{\bar{M}} \sqrt{2 + \left(\frac{m_1}{\bar{M}}\right)^2} + \frac{m_1^2}{\bar{M}^2} + 1\right), \end{aligned} \quad (20)$$

and adsorption has a weak logarithmic divergence $\Gamma \propto \ln(1/\tau)$ as the bulk critical point is approached ($\tau \rightarrow +0$).

B. Surface order-parameter

In order to analyze the surface order-parameter one needs to consider the Landau–Ginzburg–Wilson effective Hamiltonian containing extra ‘‘surface’’ contributions^{29,30}

$$\begin{aligned} H &= \frac{1}{V} \int d\vec{x}_\parallel \int_0^\infty dz (\alpha_0\tau m^2 + u_0 m^4 + c_0(\nabla m)^2 - hm \\ &\quad + b_1\delta(z)m_1^2 - h_1\delta(z)m_1), \end{aligned} \quad (21)$$

where b_1 is a surface constant and h_1 is the surface field. The procedure of minimizing of the Hamiltonian H in this case is

the same as described above, and one can obtain again the Euler–Lagrange equation Eq. (6), but with the boundary condition at the surface ($z \rightarrow 0$)

$$2c_0\left(\frac{dm(0)}{dz}\right) = 2c_0\left(\frac{dm_1}{dz}\right) = 2b_1m_1 - h_1. \quad (22)$$

At $z \rightarrow \infty$ the boundary conditions are the same as given by Eq. (7). Writing $m(0) = m_1$ and using the boundary condition Eq. (22) in Eq. (9) we obtain an equation of state for the surface,

$$\begin{aligned} 4u_0c_0(m_1 - m_b)^2[m_1^2 + 2m_b m_1 + \alpha_0\tau/u_0 + 3m_b^2] \\ = (2b_1m_1 - h_1)^2, \end{aligned} \quad (23)$$

or, using the notation introduced in the previous section, we obtain

$$\begin{aligned} \frac{h_1}{\sqrt{u_0c_0}} = \frac{2b_1}{\sqrt{u_0c_0}}m_1 + 2(m_1 - m_b) \\ \times [m_1^2 + 2m_b m_1 + \bar{\kappa} - 3m_b^2]^{1/2}. \end{aligned} \quad (24)$$

For a zero external field $m_b=0$ and Eq. (24) is transformed into expression obtained earlier by Bray and Moore,³⁰

$$\begin{aligned} h_1 = 2m_1[b_1 + \sqrt{u_0c_0}(m_1^2 + 2\bar{M}^2)^{1/2}] \\ = 2m_1[b_1 + \sqrt{c_0}(\alpha_0\tau + u_0m_1^2)^{1/2}]. \end{aligned} \quad (25)$$

III. CROSSOVER THEORY

The MF approach is valid only in the temperature region $Gi \ll |\tau| \ll 1$, where the effect of the fluctuations of the order-parameter on the thermodynamic behavior is negligibly small and all thermodynamic properties exhibit analytical classical behavior.³¹ At reduced temperatures $|\tau| \ll Gi$ the long-range fluctuations of the order parameter affect the thermodynamic properties of a system and cause them to exhibit universal scaling behavior.

In order to include the effect of the long-range fluctuations on the critical adsorption, we will use the renormalization group (RG) method and the ϵ -expansion within the self-consistent approach proposed by Rudnick and Jasnow.³² In this approach, one starts from the Landau–Ginzburg–Wilson effective Hamiltonian H as given by Eq. (4) where the order-parameter is represented as the sum of the average and fluctuation parts

$$m(z, \vec{x}_\parallel) = m + \phi(z, \vec{x}_\parallel). \quad (26)$$

The Gibbs distribution averaged value of the fluctuation part is equal to zero, $\langle \phi(z, \vec{x}_\parallel) \rangle = 0$, such that

$$\langle m(z, \vec{x}_\parallel) \rangle = m(z) = m, \quad (27)$$

and the surface value of the average part is given by

$$m(z=0) = m_1, \quad m(z \rightarrow \infty) = m_b. \quad (28)$$

After substitution of Eq. (26) in Eq. (4) the effective Hamiltonian can be written in the form

$$H \rightarrow \hat{H}^R = \frac{1}{V} \int_0^\infty dz \int d\vec{x}_\parallel (a_R m_R^2 + u_R m_R^4 + c_R (\nabla m_R)^2 - h m_R) + H_{VC}^R, \tag{29}$$

where m_R is a renormalized value of the order-parameter obtained after the integration of Eq. (4) over the wave vectors $0 < |\vec{q}| < \Lambda_0$ (where Λ_0 is the cutoff wave number), H_{VC}^R is the vacuum part of the effective Hamiltonian which does not depend on m_R . Further calculations are analogous to those used for infinite systems.^{10,20,33} The renormalized coefficients a_R and u_R to the first order of ϵ are given by

$$a_R = \alpha_0 \tau Y^{-1/3} = \alpha_0 \tau Y^{-1/3}, \quad u_R = u_0 Y^{-1}, \quad c_R = c_0. \tag{30}$$

The crossover function Y in the first order of ϵ is written in the form

$$Y = 1 - g_0 + \left(\frac{\kappa_R}{\alpha_0 Gi} \right)^{-\epsilon/2}, \tag{31}$$

$$\kappa_R = a_R + 6u_R(m - m_b)^2 + 6u_R m_b^2,$$

where

$$Gi = \left(\frac{9}{8\pi^2} \frac{k_B T_c u_0}{\epsilon \alpha_0^{2-\epsilon/2} c_0^{2-\epsilon/2}} \right)^{2/\epsilon}$$

is the Ginzburg number, k_B is the Boltzman's constant, and $g_0 = Gi^{\epsilon/2} / (\bar{\xi}_0 \Lambda_0)^\epsilon$ is a parameter dependent on the cutoff wave number Λ_0 . Since this parameter only renormalizes the background part of the isochoric specific heat at $\tau \gg Gi$ and does not change the crossover behavior of the system in the critical region,¹² we set the parameter g_0 equal to zero.²⁰

A. Crossover order-parameter profile

The equilibrium order-parameter profile $m(z)$, similar to the MF theory, is found from Eq. (5), which for the effective Hamiltonian Eq. (29) takes the form

$$\frac{\delta \hat{H}^R}{\delta m_R} = 0. \tag{32}$$

Using the translational invariance in \vec{x}_\parallel -direction and independence of a_R , u_R , and H_{VC}^R on m_R , we obtain from Eq. (32)

$$\frac{\delta \hat{H}^R}{\delta m_R} = \frac{1}{L} \int_0^\infty dz \left(2a_R m_R + 4u_R m_R^3 - 2c_0 \left(\frac{d^2 m_R}{dz^2} \right) - h \right) = 0, \tag{33}$$

which is equivalent to the equation

$$2c_0 \left(\frac{d^2 m_R}{dz^2} \right) = 2a_R m_R + 4u_R m_R^3 - h, \tag{34}$$

with the boundary conditions

$$m_R(z \rightarrow \infty) = m_b \quad \text{and} \quad \left(\frac{d^2 m_R}{dz^2} \right)_{z \rightarrow \infty} = \left(\frac{dm_R}{dz} \right)_{z \rightarrow \infty} = 0. \tag{35}$$

Integration of Eq. (34) yields

$$c_0 \left(\frac{dm}{dz} \right)^2 = a_R(m^2 - m_b^2) + u_R(m^4 - m_b^4) - h(m - m_b), \tag{36}$$

where the equilibrium value of the order parameter at given temperature τ and the ordering field h is determined from the crossover equation of state for the bulk phase

$$h = 2a_R m_b + 4u_R m_b^3. \tag{37}$$

After substitution Eq. (37) into Eq. (36) we obtain

$$c_0 \left(\frac{dm}{dz} \right)^2 = u_R \Delta m^2 [m^2 + 2m_b m + (a_R/u_R) + 3m_b^2], \tag{38}$$

where $\Delta m = m - m_b$ and the boundary condition is $m(z = 0) = m_1$.

The details of integration of Eq. (38) are given in Appendix A. The final phenomenological generalization of the crossover expression for the order-parameter profile can be represented in the form

$$z = \bar{\xi}_0 Y^{(\nu-\beta)/\Delta} \sqrt{\frac{2\bar{m}_0^2}{\kappa}} \times \ln \left[\frac{\kappa + 2m_b \Delta m + \sqrt{\kappa(\Delta m^2 + 4m_b \Delta m + \kappa)}}{\Delta m(2m_b + \sqrt{\kappa})} \right] - R_0, \tag{39}$$

$$R_0 = \bar{\xi}_0 Y_1^{(\nu-\beta)/\Delta} \sqrt{\frac{2\bar{m}_0^2}{\kappa_1}} \times \ln \left[\frac{\kappa_1 + 2m_b \Delta m_1 + \sqrt{\kappa_1(\Delta m_1^2 + 4m_b \Delta m_1 + \kappa_1)}}{\Delta m_1(2m_b + \sqrt{\kappa_1})} \right], \tag{40}$$

$$\kappa = 2\bar{m}_0^2 \tau Y^{(1-2\beta)/\Delta} + \omega_3 m_b^2 = \pm 2M^2 \left(\frac{Y}{Y_b} \right)^{(1-2\beta)/\Delta} + \omega_3 m_b^2, \tag{41}$$

$$\kappa_1 = 2\bar{m}_0^2 \tau Y_1^{(1-2\beta)/\Delta} + \omega_3 m_b^2 = \pm 2M^2 \left(\frac{Y_1}{Y_b} \right)^{(1-2\beta)/\Delta} + \omega_3 m_b^2, \tag{42}$$

where the signs “+” and “-” correspond to the high ($\tau > 0$) and low ($\tau < 0$) temperature region, respectively. The crossover functions Y , Y_1 , and Y_b are given by

$$Y = 1 - g_0 + Y^{(\gamma-2\beta)/\gamma} \left[\frac{1}{Gi} \left(\tau Y^{(1-2\beta)/\Delta} + \omega_1 \left(\frac{\Delta m}{\bar{m}_0} \right)^2 + \omega_2 \left(\frac{m_b}{\bar{m}_0} \right)^2 \right) \right]^{-\Delta/\gamma}, \tag{43}$$

$$Y_1 = 1 - g_0 + Y_1^{(\gamma-2\beta)/\gamma} \left[\frac{1}{Gi} \left(\tau Y_1^{(1-2\beta)/\Delta} + \omega_1 \left(\frac{\Delta m_1}{\bar{m}_0} \right)^2 + \omega_2 \left(\frac{m_b}{\bar{m}_0} \right)^2 \right) \right]^{-\Delta/\gamma}, \tag{44}$$

$$Y_b = 1 - g_0 + Y_b^{(\gamma-2\beta)/\gamma} \times \left[\frac{1}{Gi} \left(\tau Y_b^{(1-2\beta)/\Delta} + \omega_2 \left(\frac{m_b}{m_0} \right)^2 \right) \right]^{-\Delta/\gamma} \quad (45)$$

In Eqs. (39)–(45), $M = \bar{m}_0 |\tau|^{1/2} Y_b^{(1-2\beta)/2\Delta} = m_0 |\tau|^\beta \times (|\bar{\tau}|^\Delta Y_b)^{(1-2\beta)/2\Delta}$ is the order-parameter at the coexistence curve; $\bar{\tau} = \tau/Gi$ is the rescaled temperature; $m_0 = \bar{m}_0 Gi^{1/2-\beta}$ is the asymptotic critical amplitude; $\gamma = 1.24$, $\beta = 0.325$, and $\Delta = 0.51$ are the current best estimates of the nonclassical critical exponents, and ω_i ($i = 1, 2, 3$) are the universal constants. In the zero external field the bulk order-parameter $m_b = 0$, and Eqs. (39)–(45) are transformed into the crossover expressions for the order parameter profile and the crossover functions obtained earlier by Belyakov *et al.*,^{20,21} and the constant $\omega_1 = \omega = 0.51$. The crossover equation of state Eq. (37) and the bulk crossover function Y_b as given by Eq. (45) exactly correspond to ones in the crossover Leung–Griffiths model,³⁴ and the constant $\omega_2 = \lambda_1/2 = 4.39$ is directly related to the universal constant λ_1 in Ref. 34. In the temperature region $Gi \ll \tau \ll 1$ at $m_b = 0$ and the density region $m_0 Gi^\beta \ll |m_b| \ll 1$ at $\tau = 0$ the crossover functions Y and Y_1 tend to one ($Y \cong Y_1 \cong 1$) and crossover Eqs. (39)–(42) with $\omega_3 = 6$ are exactly transformed in the MF expressions (12)–(14).

In the zero external field Eqs. (39) and (40) can be represented in universal form,²¹

$$m(z) = m_0 \tau^\beta \hat{P}_+(x), \quad (46)$$

where

$$x = \frac{z}{\xi_b} \left(\frac{Y_b}{Y} \right)^{(2\nu-1)/2\Delta} = \zeta \left(\frac{Y_b}{Y} \right)^{(2\nu-1)/2\Delta}, \quad (47)$$

$$x_0 = \frac{R_0}{\xi_b} \left(\frac{Y_b}{Y} \right)^{(2\nu-1)/2\Delta},$$

and the universal order-parameter profile crossover function

$$\hat{P}_+(x) = (\bar{\tau}^\Delta Y)^{(1-2\beta)/2\Delta} \frac{\sqrt{2}}{\sinh(x+x_0)} \quad (48)$$

[unlike the universal function $P_+(\zeta)$ in Eq. (2)] is not a universal function of the parameter ζ alone, even in the critical regime at $\tau \ll Gi$. The detailed analysis of the asymptotic behavior of the crossover function $\hat{P}_+(x)$ is given in Ref. 21. The main result of this analysis is that in case of infinite adsorption ($m_1 \rightarrow \infty$ and $x_0 = 0$), near the wall at distances $0 \leq z \leq \xi_0 Gi^{-\nu}$ (or $0 \leq \zeta \leq \zeta_0$, where $\zeta_0 = \bar{\tau}^\nu$ is a characteristic length) the scaling function $\hat{P}_+(x)$ exhibits the mean field behavior

$$\hat{P}_+(x) = \bar{P}_0 \bar{z}^{-1}. \quad (49)$$

This result has a simple physical explanation. Since the infinite adsorption corresponds to the condition $h_1 \rightarrow \infty$ [see Eq. (25)], the surface field suppresses the fluctuations of the order-parameter near the wall, causing them to exhibit the

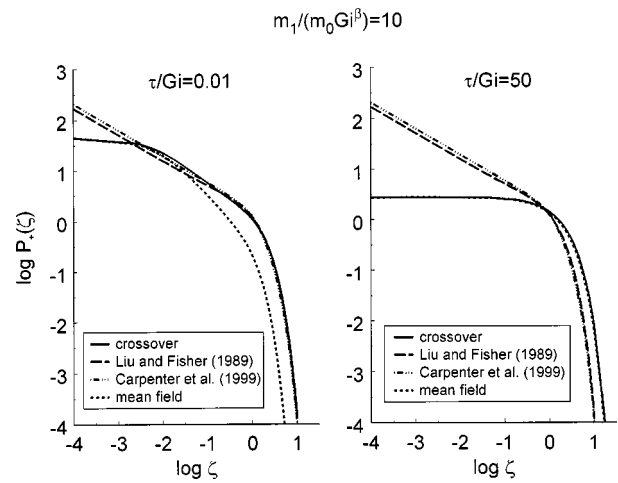


FIG. 1. Scaling function P_+ for the order-parameter profile as a function of the dimensionless distance ζ . The solid curve calculated with the crossover Eq. (48), the long-dashed curve was generated with the Liu and Fisher model (Ref. 35), the dotted-dashed curve represents an empirical model of Carpenter *et al.* (Ref. 36), and the short-dashed curve corresponds to the mean-field approximation.

mean-field behavior. At distances $\zeta \gg \zeta_0$, the scaling function $\hat{P}_+(x)$ obeys the Fisher–deGennes scaling hypothesis as given by Eq. (3).

In Fig. 1 we show a comparison of our crossover function \hat{P}_+ for the case of strong adsorption, $m_1/(m_0 Gi^\beta) = 10$, with the Pade approximate for the scaling function P_+^{FdG} proposed by Liu and Fisher³⁵ and with the empirical scaling function obtained recently by Carpenter *et al.*³⁶ As one can see, in the scaling regime at $\bar{\tau} = 10^{-2}$ the characteristic length $\zeta_0 = 5.6 \times 10^{-2}$ and at $\zeta \leq 5.6 \times 10^{-2}$ ($\log \zeta \leq -1.25$) our crossover function $\hat{P}_+(x)$, unlike the scaling functions of Liu and Fisher³⁵ and of Carpenter *et al.*,³⁶ does exhibit the MF behavior. At distances $\zeta \gg 5.6 \times 10^{-2}$ ($\log \zeta \gg -1.25$) all three scaling functions practically coincide. At rescaled temperature $\bar{\tau} = 50$, the characteristic length $\zeta_0 = 11.5$ and the MF behavior of the order-parameter profile is observed into the entire region $0 < \zeta < 10$.

B. Critical adsorption

In the case of the crossover order-parameter profile as given by Eqs. (39) and (40), the integral on the right side of Eq. (18) for the adsorption cannot be expressed as a finite combination of elementary functions. Therefore, no rigorous analytic expression for the adsorption can be obtained in this case. In our previous work^{20,21} we discussed a reasonable analytic approximation for the adsorption for the zero external field, at $m_b = 0$. Here we have generalized this expression for nonzero external field.

In order to analyze the adsorption analytically it is better to start from Eq. (18). The minimum of the free-energy functional of the system with the effective Hamiltonian Eq. (29) corresponds to the negative root of Eq. (38)

$$\left(\frac{dm}{dz} \right) = - \sqrt{\frac{u_R}{c_0}} (m - m_b) \sqrt{m^2 + 2m_b m + \frac{a_R}{u_R} + 3m_b^2}. \quad (50)$$

After substitution of Eq. (50) into Eq. (18) with the boundary condition $m(z=0)=m_1$ we have for the adsorption

$$\Gamma = \sqrt{\frac{c_0}{u_0}} \times \int_0^{\Delta m_1} \frac{Y^{1/2} d(m-m_b)}{\sqrt{(m-m_b)^2 + 4m_b(m-m_b) + 2\bar{m}_0\tau Y^{2/3} + 6m_b^2}} \quad (51)$$

Equation (51) can also be integrated rigorously only numerically, but we can obtain a good approximation for this integral. The analytical estimate of the integral at the right side of Eq. (51) obtained in the first order of ϵ and its phenomenological generalization are given in Appendix B.

Finally, the crossover expression for the adsorption can be written in the form

$$\Gamma = \frac{\bar{m}_0\bar{\xi}_0}{\sqrt{2}} Y_1^{(\nu-\beta)/\Delta} \ln \left[\frac{m_1 + m_b + \sqrt{m_1^2 + 2m_b m_1 - 3m_b^2 + \kappa_1}}{\bar{m}_0 \sqrt{2\kappa_1/\bar{\kappa}}} \right]^2 - \frac{\bar{m}_0\bar{\xi}_0}{\sqrt{2}} Y_b^{(\nu-\beta)/\Delta} \ln \left[\left(\frac{Y_1}{Y_b} \right)^{(1-2\beta)/2\Delta} \frac{2m_b + \sqrt{\kappa_b}}{\bar{m}_0 \sqrt{2\kappa_1/\bar{\kappa}}} \right]^2, \quad (52)$$

where

$$\kappa_b = 2\bar{m}_0^2\tau Y_b^{(1-2\beta)/\Delta} + \omega_3 m_b^2 = \pm 2M^2 + \omega_3 m_b^2. \quad (53)$$

In the zero external field at $\tau \geq 0$ the bulk order-parameter $m_b=0$, $\kappa_b = 2\bar{m}_0^2\tau Y_b^{(1-2\beta)/\Delta} = 2M^2$, $\kappa_1 = 2\bar{m}_0^2\tau Y_1^{(1-2\beta)/\Delta} = 2M^2(Y_1/Y_b)^{(1-2\beta)/\Delta}$, the product $\bar{m}_0\bar{\xi}_0 Y_b^{(\nu-\beta)/\Delta} = M\xi_b$, and Eq. (52) exactly correspond to the crossover expression for the adsorption obtained earlier by Kiselev *et al.*²¹ In the zero external field, at $m_b=0$, $\tau \ll Gi$ ($\bar{\tau} \ll 1$), and $m_1 = \text{const}$, the adsorption diverges as $\Gamma \propto \xi_b M \propto \tau^{-\nu+\beta}$ approaching the critical temperature.²¹ In the MF regime ($Gi \ll \tau \leq 1$ at $m_b=0$, and $Gi^\beta \ll |m_b| \leq 1$ at $\tau=0$), the crossover functions $Y_1 \rightarrow 1$ and $Y_b \rightarrow 1$, the parameters $\kappa_b \rightarrow \bar{\kappa}$ and $\kappa_1 \rightarrow \bar{\kappa}$, and the crossover Eq. (52) is transformed into the MF expression Eq. (19).

It is interesting to compare the values for the adsorption calculated with Eq. (52) with the result of the numerical integration of Eq. (18). For this aim it is useful to rewrite Eq. (18) in the form

$$\Gamma = \int_0^\infty \Delta m dz = \Delta m z|_0^\infty - \int_{\Delta m_1}^0 z(\Delta m) d\Delta m = \int_0^{\Delta m_1} z(\Delta m) d\Delta m, \quad (54)$$

where for the order-parameter profile $z(\Delta m)$ one can use the phenomenological generalization as given by Eq. (39). For a comparison we choose a system with $Gi=0.01$, $m_0=m_1=1$, and $\xi_0=0.2$ nm. The values of adsorption calculated from Eq. (52) in comparison with results of numerical integration of Eq. (54) for this case are shown in Fig. 2. Qualitatively, both methods give similar behavior of the adsorption in the critical region. However, for $|m_b| \leq 0.2$ at

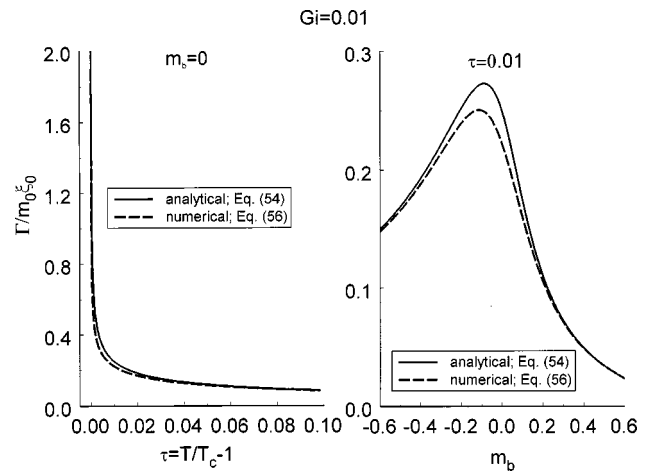


FIG. 2. Adsorption as a function of the dimensionless temperature τ (left) and as a function of the bulk order-parameter m_b (right). The solid lines correspond to the values calculated with Eq. (52) and the dashed curves represent the values obtained with a numerical integration of Eq. (54).

temperatures $\tau \leq 0.01$, some quantitative discrepancy between numerical integration and values calculated from Eq. (52) is observed. Therefore, in order to avoid a possible misinterpretation of the experimental data, our analysis of the critical adsorption data will be performed using numerical integration of Eq. (54).

IV. COMPARISON WITH EXPERIMENTAL DATA

In order to use this model for a comparison with experimental data for the surface excess, or Gibbs, adsorption, one needs to know the bulk critical parameters of the system, T_c and ρ_c for pure fluids, the asymptotic critical amplitude of the coexistence curve, m_0 , and of correlation length, ξ_0 , and the Ginzburg number Gi . All these parameters can be obtained from the independent analysis of the bulk properties of the system in the critical region. The corresponding MF critical amplitudes \bar{m}_0 and $\bar{\xi}_0$ in Eqs. (39) and (40) can be calculated using relations

$$\bar{m}_0 = m_0 Gi^{\beta-1/2}, \quad \bar{\xi}_0 = \xi_0 Gi^{\nu-1/2}. \quad (55)$$

The surface appears in Eqs. (39) and (40) only through the surface order-parameter m_1 . Therefore, in addition to the bulk properties of the system, one needs also to know the equation of state for the surface. Since in the case of the strong adsorption (at $m_1 > m_0 Gi^\beta$) in the limit $z \rightarrow 0$ we always have the MF behavior of the order-parameter profile, we can use Eq. (24) for this purpose. The parameters u_0 , α_0 , and c_0 in this equation related to the parameters m_0 , ξ_0 , and Gi as

$$u_0 = \frac{9}{32\pi^2} \frac{k_B T_c}{m_0^4 \xi_0^3 Gi^{4\beta-3\nu}}, \quad \alpha_0 = 2m_0^2 Gi^{2\beta-1} u_0, \quad (56)$$

$$c_0 = \alpha_0 Gi^{1-2\nu} (\rho_c^{1/3} \xi_0)^2.$$

In addition, we assume that the system-dependent parameter $b_1 = b_{10} \sqrt{u_0 c_0}$, where b_{01} is a temperature independent constant, while the surface field h_1 is treated as an analytic function of temperature

$$\frac{h_1}{\sqrt{u_0 c_0}} = h_{10} + \sum_{i=1} h_{1i} \tau^i, \quad (57)$$

where h_{1i} are the system-dependent constants. Thus, in order to describe experimental data for the Gibbs adsorption in real systems, one needs to know the bulk properties and the surface parameters b_{10} and h_{1i} ($i=0,1,\dots$).

The first system, to which the crossover model was optimized, is supercritical carbon dioxide on octadecyl-bonded silica. The surface excess adsorption in this system has been measured by Strubinger and Parcher²² at different pressures along three isotherms $T = 303.15, 313.15,$ and 323.15 K. In order to transform these data into $T-\rho$ coordinates we used the parametric crossover equation of state (EOS) for CO_2 developed by Kiselev and Kulikov.³⁷ This crossover EOS, similar to our crossover model for adsorption, reproduces the singular behavior of the thermodynamic properties in the critical region at $|\tau| \ll Gi$, and at $|\tau| \gg Gi$ is transformed into the classical mean-field EOS. Good representation of the thermodynamic properties of pure CO_2 with the crossover EOS was achieved in the range of temperatures and densities bounded by³⁷

$$0.995T_c \leq T \leq 1.4T_c, \quad 0.35\rho_c \leq \rho \leq 1.65\rho_c. \quad (58)$$

In contrast to our crossover model, the crossover EOS of Kiselev and Kulikov³⁷ contains additional terms which take into account an asymmetry of real fluids with respect to the critical isochore.³⁸ Therefore, we expect that our symmetric crossover model, similar to the symmetric scaled EOS for pure fluids, can be applied in the range of temperatures and densities not wider than³⁹

$$0.995T_c \leq T \leq 1.15T_c, \quad 0.5\rho_c \leq \rho \leq 1.5\rho_c. \quad (59)$$

After this elimination, only six points from the experimental data of Strubinger and Parcher²² on two isotherms ($T = 313.15$ and 323.15 K) were left. These points, together with additional five points on the $T = 313.15$ K isotherm obtained in Ref. 23, are shown in Fig. 3. As one can see, there is some discrepancy between two data sets at $\rho/\rho_c > 1$; therefore, for further numerical analysis we used here only data reported in Ref. 22.

In the critical region at $Gi \ll \tau \ll 1$, the parametric crossover model employed by Kiselev and Kulikov³⁷ exactly corresponds to the MF EOS as given by Eq. (8) with the order-parameter

$$m_b = \Delta\rho - d_1 \tau, \quad (60)$$

where $\Delta\rho = \rho/\rho_c - 1$, d_1 is a rectilinear diameter amplitude of the coexistence curve, the external field is a dimensionless chemical potential of the fluid.^{40,41} Therefore, the parameters α_0 and u_0 in the MF EOS are directly related to the parameters k , a , and g in the parametric crossover model³⁷ (for

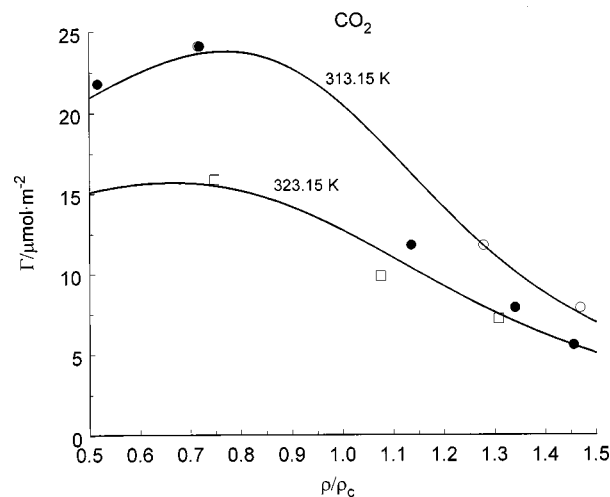


FIG. 3. Surface excess adsorption of CO_2 on octadecyl-bonded silica at $T = 313.15$ and 323.15 K as a function of density. The empty symbols represent experimental data of Strubinger and Parcher,²² the filled symbols correspond to data from Ref. 23 and the curves represent the values calculated with the crossover model.

details see Refs. 40, 41). For the asymptotic critical amplitude of the coexistence curve m_0 and the Ginzburg number Gi we obtained

$$m_0 = \frac{k}{(b^2 - 1)^\beta},$$

$$Gi = g^{-1} \frac{b^2 - 1}{2[2(b^2 - 1) + (2\gamma - 1)(2 - \alpha)]/\gamma(1 - \alpha)}^{1/(1 - 2\beta)}, \quad (61)$$

where b^2 is a universal linear-model parameter.

For pure CO_2 we adopt the same critical parameters,

$$T_c = 304.136 \text{ K}, \quad \rho_c = 10.625 \text{ mol} \cdot \text{L}^{-1},$$

$$P_c = 7.3773 \text{ MPa}, \quad (62)$$

and the values of the bare correlation length ξ_0 and rectilinear diameter amplitude d_1 ,

$$\xi_0 = 0.15 \text{ nm}, \quad d_1 = -0.9221, \quad (63)$$

as reported by Kiselev and Kulikov,³⁷ while the parameters

$$m_0 = 1.708 \quad \text{and} \quad Gi = 0.115, \quad (64)$$

were calculated from Eqs. (61) with the parameters $k = 1.2245$ and $g = 0.1477$ taken from Ref. 37. Six points on two isotherms are not enough for the statistical optimization procedure. Therefore, initially we set $b_{10} = 1$ and $h_{10} = 10$, to provide a condition $m_1/(m_0 Gi^\beta) \cong 2$, while the parameter $h_{11} = -39.51$ was found from a fit of our model to the excess adsorption data of Strubinger and Parcher.²² Comparison of the experimental data with the values of the Gibbs adsorption calculated with the crossover model is given in Fig. 3. Good agreement between experimental data and the predicted values is observed in the range of temperatures and densities as given by Eq. (59).

In principle, the range of the validity of the model can be extended. A theoretically consistent way of extending of the

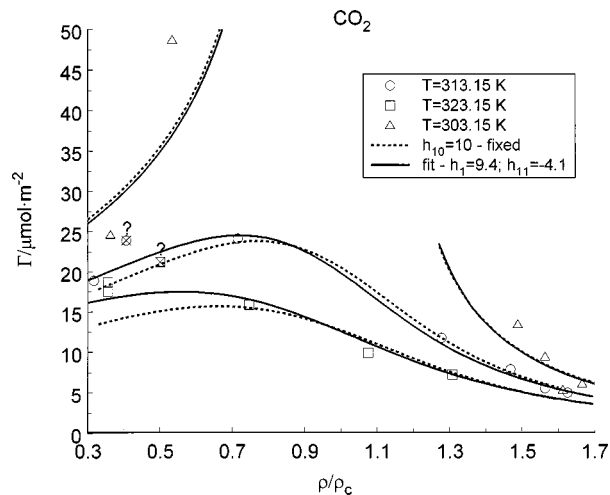


FIG. 4. Surface excess adsorption of CO₂ on octadecyl-bonded silica along isotherms in the extended density region. The symbols represent experimental data of Strubinger and Parcher,²² the dashed curves correspond to the values obtained from Eq. (54) with $h_{10}=10$, and the solid curves represent the values calculated with Eq. (54) with the parameters h_{10} and h_{11} found from a fit to the experimental data.

model to a wider density range is to consider the asymmetric terms in the effective Hamiltonian of the system (see, for example, Refs. 42, 43). However, this approach needs additional theoretical study which is not the subject of the present work. In the present article, we improved the model by fitting both parameters, h_{10} and h_{11} , to experimental data. Finally, for this system we adopt the values

$$b_{10}=1, \quad h_{10}=9.744, \quad h_{11}=-4.107. \quad (65)$$

The results of the fit are shown in Fig. 4. Except two points marked in Fig. 4 by a cross, the model yields a good representation of all experimental data in the range of densities $0.3 \leq \rho/\rho_c \leq 1.7$.

There are no surface excess adsorption data for the CO₂/silicia system along the critical isochore of CO₂. Therefore, in Fig. 5 we show a comparison of the values of the

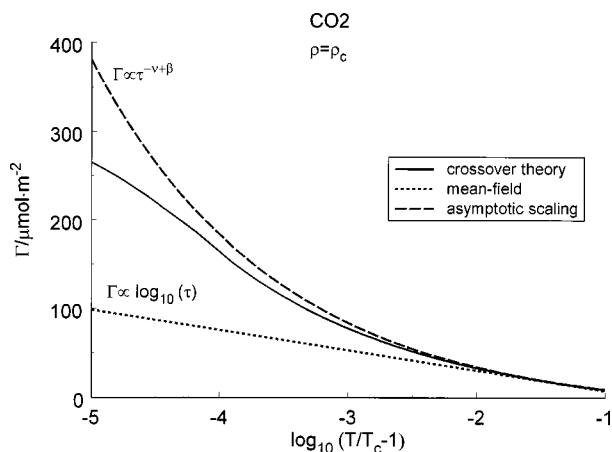


FIG. 5. Surface excess adsorption of CO₂ on octadecyl-bonded silica along the critical isochore as a function of temperature. The solid curve represents the values generated with the crossover model, the short-dashed curve corresponds to the MF Eq. (20), and the long-dashed curve represents the values calculated with asymptotic Eq. (66).

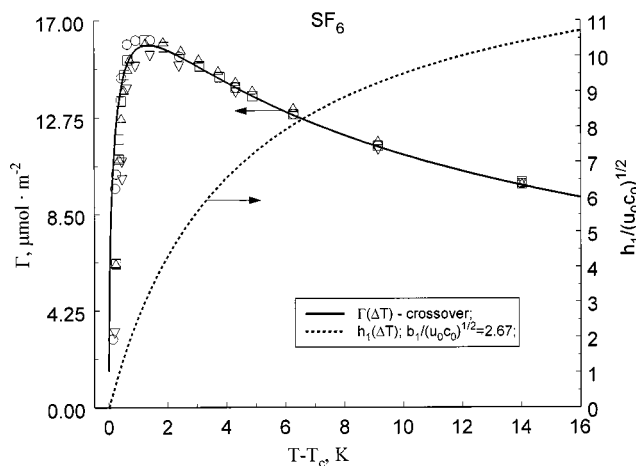


FIG. 6. Surface excess adsorption of SF₆ on graphitized carbon (left) and the surface field h_1 (right) along the critical isochore as a function of temperature. The symbols represent experimental data of Thommes *et al.* (Ref. 24) and the curves represent the values calculated with the crossover model.

Gibbs adsorption of CO₂ calculated at the critical isochore with the crossover model with the values calculated with the MF Eq. (20) and with the asymptotic scaling expression

$$\Gamma = A \tau^{-\nu+\beta} + B, \quad (66)$$

where A and B are the system dependent coefficients. Equations (20) and (66) were optimized to the Gibbs adsorption data generated with the crossover model at $\rho = \rho_c$ and $0.05 \leq \tau \leq 0.1$. As one can see, even though at $\tau \approx 0.1$ all three models practically coincide, the difference between them increases dramatically as $\tau \rightarrow 0$. In reality, the MF model optimized to experimental data far from the critical region is unable to reproduce the Gibbs adsorption data in the region where $\tau \leq 0.1$. This is a reason why such analytical mean-field theories such as the BET⁴ or the local density model⁵⁻⁷ cannot be extrapolated in the critical region at $\tau \rightarrow 0$ ($\tau \ll Gi$).

The second system, which has been considered here is near-critical SF₆ on a graphite substrate. The detailed experimental critical adsorption data in this system have been obtained by Thommes *et al.*²⁴ not only along isotherms, but also along isochores as a function of temperature. It makes this system extremely attractive for the testing of the theory. In addition, the anomalous behavior of the adsorption on the critical isochore observed in the experiment presents a real challenge for the model.²¹

The experimental critical adsorption data obtained by Thommes *et al.*²⁴ at the critical density of pure SF₆ are shown in Fig. 6. Unlike the theoretical prediction (see Fig. 2), the adsorption in this system increases only down to reduced temperatures $\tau \approx 0.01$ ($\Delta T \approx 2$ K) but then Γ decreases sharply on approaching T_c . In the previous work we have shown that this anomalous behavior of the adsorption along the critical isochore can be treated by supposing that the surface order-parameter profile vanishes linearly with τ .²¹

In this article, we analyzed experimental data of Thommes *et al.*²⁴ in two steps. Firstly, we considered experi-

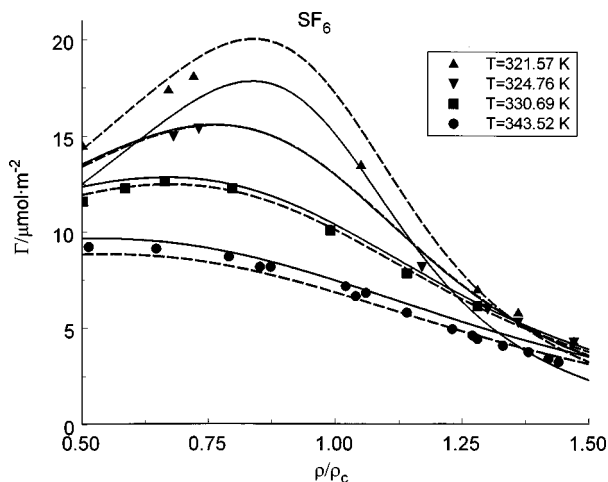


FIG. 7. Surface excess adsorption of SF₆ on graphitized carbon along the isotherms as a function of density. The solid curves represent the values calculated with the crossover model with parameters as given in Eq. (69), the dashed curves correspond to the values calculated with parameters given in Eq. (70), and symbols represent experimental data of Thomess *et al.* (Ref. 24).

mental data at the critical isochore only. Similar to our previous work,²¹ for the bulk SF₆ we adopt the parameters

$$Gi = 2.1 \times 10^{-2}, \quad m_0 = 1.715, \quad d_1 = -0.9488, \quad (67)$$

obtained by Ley-Koo and Green⁴⁴ (parameters t_{\max} , B_0 , and $-b$ in Ref. 44), for $\xi_0 = 0.2$ nm, we adopt the value obtained by Sengers and Levelt Sengers,⁴⁵ while the surface order-parameter m_1 was calculated from Eq. (24) with the surface field

$$h_1 = f_0 + f_1 f_s(\tau/\tau_1), \quad (68)$$

where $f_s(\vartheta) = \vartheta/(1+\vartheta)$ is a function introduced in Ref. 21. From a fit of the crossover model to the experimental data at the critical isochore only, we found that parameter f_0 is statistically irrelevant and can be set equal zero, and the parameters

$$b_{10} = 2.67, \quad f_1 = 13.6, \quad \tau_1 = 1.35 \times 10^{-2}. \quad (69)$$

In Fig. 6 we show a comparison of experimental excess adsorption data obtained at the critical isochore by Thommes *et al.*²⁴ with the values calculated with the crossover model. Excellent agreement of the calculated values with experimental data is observed. In the same figure we show the surface field h_1 as a function of the temperature difference $\Delta T = T - T_c$. At $\Delta T = 16$ K ($\tau \approx 0.05$), similar to the system considered above, $h_1/\sqrt{u_0 c_0} \approx 10$. However, in contrary to this system, at the surface field $h_1 \rightarrow 0$ as the critical temperature is approaching. It is interesting to compare the prediction of the theory in this case with other experimental data obtained in Ref. 24. A comparison of the excess adsorption isotherms obtained by Thommes *et al.*²⁴ with the values calculated with our crossover model is shown in Fig. 7. In the density range $0.5 \leq \rho/\rho_c \leq 1.5$ at temperatures $T \geq 324$ K ($\tau \geq 0.02$) the crossover theory gives a good representation of experimental data. However, at $T = 321.57$ K the systematic

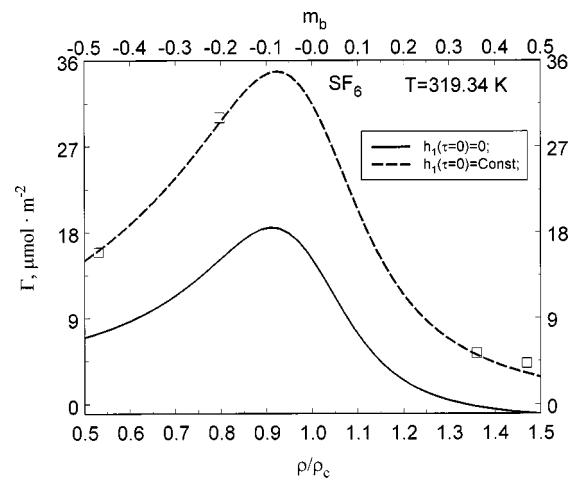


FIG. 8. Surface excess adsorption of SF₆ on graphitized carbon along the near-critical isotherm $T = 319.34$ K as a function of density. The solid curve represents the values calculated with the crossover model with the parameters given in Eq. (69), the dashed curve corresponds to the values calculated with parameters given in Eq. (70), and symbols represent experimental data of Thomess *et al.* (Ref. 24).

deviations of the calculated values from experimental data are observed which increase up to 50%–70% at the near-critical isotherm $T = 319.34$ K (see Fig. 8).

In Fig. 9 we show a comparison of the experimental and calculated values of the adsorption along the noncritical isochores. As one can see, the crossover theory in this case even qualitatively does not reproduce experimental data in the near critical region at $\Delta T < 4$ – 6 K ($\tau \leq 0.02$). Therefore, as a second step, we used for the external field h_1 the MF Eq. (24). Similar to the CO₂/silicia system, the parameters

$$b_{10} = 2.07, \quad h_{10} = 4.47, \quad h_{11} = 1.39 \times 10^2, \quad (70)$$

$$h_{12} = -1.05 \times 10^3,$$

for SF₆/graphite system were found from a fit of the crossover model only to the surface excess isotherms. The values of the adsorption calculated with the crossover model with

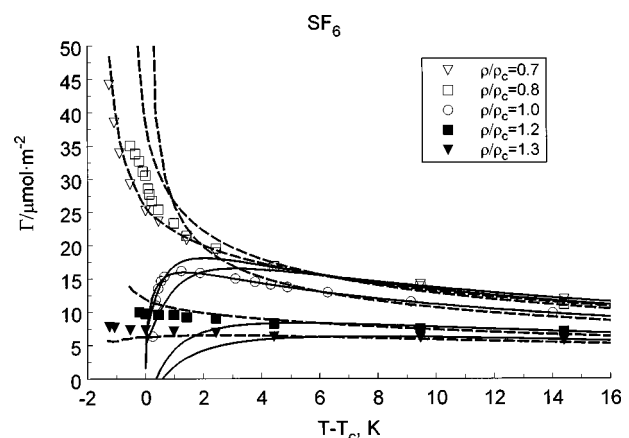


FIG. 9. Surface excess adsorption of SF₆ on graphitized carbon along the isochores as a function of temperature. The solid curves represent the values calculated with the crossover model with parameters given in Eq. (69), the dashed curves correspond to the values calculated with parameters given in Eq. (70), and symbols represent experimental data of Thommes *et al.* (Ref. 24).

these parameters correspond to the dashed curves in Figs. 7–9. Because of the absence of the tables with real experimental data in Ref. 24, the points in Figs. 7–9 represent the values obtained with a graphical interpolation from Figs. 1, 3, and 4 of Ref. 24. It explains some inconsistency between experimental data presented in Figs. 8 and 9 at $T=319.34$ K and $\rho/\rho_c=0.8$. In general, with the parameters given in Eq. (70), the crossover model, except the temperatures $\tau\leq 0.02$ at $\rho=\rho_c$, yields a reasonably good representation of all experimental data in the range of temperatures and densities as given by Eq. (59).

V. DISCUSSION

We developed the crossover theory for the surface excess adsorption of pure fluids on the solid surface. Similar to crossover theory for the bulk properties,^{12,13} our crossover theory for the adsorption contains the Ginzburg number, Gi , as a parameter. Along the critical isochore the crossover expression for the order-parameter profile can be written in the universal form proposed by Fisher and de Gennes.³ In the asymptotic critical region at dimensionless temperatures $|\tau|\ll Gi$ and distances $z\gg\xi_0 Gi^{-\nu}$, the universal crossover function for the order-parameter profile exhibits singular behavior and obeys the Fisher–deGennes scaling hypothesis.³ At distances $0\leq z\leq\xi_0 Gi^{-\nu}$, and in the temperature range $Gi\ll|\tau|\leq 1$ the universal crossover function is transformed into the well-known MF expression for the order-parameter profile in the semiinfinite system.¹⁶

The crossover theory was tested against experimental data for adsorption of supercritical carbon dioxide on octadecyl-bonded silica measured by Strubinger and Parcher²² and against the surface excess adsorption data in near-critical SF₆ on a graphite substrate obtained by Thommes *et al.*²⁴ For the CO₂/silica system, a good agreement between the theoretical predictions and experimental data is observed. For the SF₆/graphite system, only a moderate success was achieved. The main challenge for the modelling of this system is an anomalous decreasing of the adsorption along the critical isochore on approaching the bulk critical temperature T_c .²⁴

In our previous article,²¹ we have shown that this anomalous behavior of the adsorption can be described accurately in the framework of the crossover theory with the surface order-parameter profile vanishing linearly at $\tau\rightarrow 0$. In this work, we calculated the surface order-parameter m_1 from the MF surface equation of state [Eq. (24)]. A theoretical study of this equation has been performed by Lubensky and Rubin²⁹ and by Bray and Moore.³⁰ It has been shown that at $h=0$ and $h_1=0$ Eq. (24) gives three classes of the surface phase transitions.^{29,30} The *ordinary* transition occurs at $\tau=0$ and $b_1>0$, the *extraordinary* transition occurs at $\tau=0$ and $b_1<0$, and these transitions are separated by the *special* transition at $\tau=0$ and $b_1=0$. In addition, the *normal* surface transition occurs on the surface as a result of $h_1\neq 0$ and $b_1>0$.⁴⁶ It has been argued⁴⁷ that a fluid against a hard wall has surface critical behavior in the universality class of *normal* transition. The results of the optimization of the model to the excess isotherms in the CO₂/silica and in SF₆/graphite systems are in a complete agreement with this

conclusion. However, in this case theory fails to reproduce the excess adsorption data for SF₆/graphite system at temperatures $\tau\leq 0.02$ at $\rho=\rho_c$. We found that an excellent agreement with excess adsorption data along the critical isochore in SF₆/graphite system is achieved, if the surface coupling constant $b_1>0$ and the surface field $h_1\rightarrow 0$ as $\tau\rightarrow 0$, which corresponds to the *ordinary* transition. However, in this case the theory fails to reproduce the excess isotherms at $|\tau|<0.02$. We cannot say for sure what causes the SF₆/graphite system to exhibit such anomalous behavior. To answer this question, the additional theoretical and experimental study is needed.

In developing crossover expressions for the order-parameter profile, we used a field-theoretical approach based on the Landau–Ginzburg–Wilson effective Hamiltonian given by Eq. (21). This is a general approach, and the crossover function for the semiinfinite system obtained in this article (which is similar to the crossover function for the bulk properties obtained earlier by Belyakov and co-workers^{12,14}) can be applied to any system with a scalar order-parameter. Recent research indicates that such complex systems as aqueous ionic solutions,³⁴ polymers and polymer blends,^{48–52} and microemulsions⁵³ can be described in the critical region with the crossover function obtained by Belyakov and Kiselev,¹² where the Ginzburg number, Gi , depends on the composition (for ionic solutions) or on the molecular weight (for polymers). Therefore we expect that the crossover equations obtained in this work can be also applied for the analysis of critical adsorption data in binary liquid mixtures and in complex fluids in general. Research toward the application of this crossover approach to other systems is in progress, and the results will be presented in future publications.

ACKNOWLEDGMENTS

The authors are indebted to M.E. Fisher for his interest in this work and constructive comments. The research was supported by the Office of Basic Energy Sciences of the U.S. Department of Energy under Grant No. DE-FG03-95ER14568.

APPENDIX A: CROSSOVER EXPRESSION FOR ORDER-PARAMETER PROFILE

Equation (50) can be written in the integral form

$$\int_m^{m_1} \sqrt{\frac{c_0}{u_R}} \frac{dx}{(x-m_b)\sqrt{x^2+2m_b x+(a_R/u_R)+3m_b^2}} = -\int_z^0 dz = z. \quad (\text{A1})$$

The integral on the left side of Eq. (A1) can only be evaluated numerically. In order to estimate this integral analytically let us introduce a notation $\hat{x}=(x-m_b)/(\sqrt{2}\bar{m}_0)$. Then Eq. (A1) reads

$$z = \int_{\hat{m}}^{\hat{m}_1} \sqrt{\frac{c_0 Y}{\alpha_0 \hat{x} \sqrt{\hat{x}^2 + 4\hat{m}_b \hat{x} + \hat{\kappa}}}} d\hat{x} \\ = \int_{\hat{m}}^{\hat{m}_1} \frac{\sqrt{\frac{c_0}{\alpha_0 \tilde{\kappa}} \left(\frac{1}{\sqrt{\tilde{\kappa}}} d\hat{x} \right)}}{\frac{\hat{x}}{\sqrt{\tilde{\kappa}}} \sqrt{\left(\frac{\hat{x}}{\sqrt{\tilde{\kappa}}} \right)^2 + 4 \left(\frac{\hat{m}_b}{\sqrt{\tilde{\kappa}}} \right) \left(\frac{\hat{x}}{\sqrt{\tilde{\kappa}}} \right) + 1}}, \quad (\text{A2})$$

where

$$\hat{m} = (m - m_b) / (\sqrt{2\bar{m}_0}), \quad \hat{m}_1 = (m_1 - m_b) / (\sqrt{2\bar{m}_0}), \quad (\text{A3})$$

$$\hat{m}_b = m_b / (\sqrt{2\bar{m}_0}),$$

$$\hat{\kappa} = \tau Y^{2/3} + 6\hat{m}_b^2, \quad \tilde{\kappa} = Y^{-1} \hat{\kappa} = \tau Y^{-1/3} + 6\hat{m}_b^2 Y^{-1}, \quad (\text{A4})$$

and to the first order of ϵ the crossover function

$$Y = 1 - g_0 + Y^{\epsilon/2} \left[\frac{\hat{\kappa} + 6\hat{x}^2}{Gi} \right]^{-\epsilon/2}. \quad (\text{A5})$$

Let introduce a variable $\theta = \hat{x} / \sqrt{\tilde{\kappa}}$, such that

$$d\theta = \frac{d}{d\hat{x}} \left(\frac{\hat{x}}{\sqrt{\tilde{\kappa}}} \right) d\hat{x} = \frac{1}{\sqrt{\tilde{\kappa}}} d\hat{x} \left[1 - \frac{\hat{x} Y^{-1}}{3} \cdot \frac{\tau Y^{2/3}}{\hat{\kappa}} \left(\frac{dY}{d\hat{x}} \right) \right], \quad (\text{A6})$$

and substitute the derivative $(dY/d\hat{x})$ in Eq. (A6) with the expression obtained from Eq. (A5) to the first order of ϵ

$$d\theta = \frac{1}{\sqrt{\tilde{\kappa}}} d\hat{x} \\ \times \left(1 + \frac{2\epsilon}{[1 - (\epsilon/2)Q]} \cdot \frac{(Y-1+g_0)}{Y} \cdot \frac{\tau Y^{2/3}}{\hat{\kappa}} \cdot \frac{\hat{x}^2}{(\hat{\kappa} + 6\hat{x}^2)} \right) \\ = \frac{1}{\sqrt{\tilde{\kappa}}} d\hat{x} (1 + \mathcal{O}(\epsilon)) \approx \frac{1}{\sqrt{\tilde{\kappa}}} d\hat{x}, \quad (\text{A7})$$

where $Q = (1 - 2a_R/3\kappa_R)(Y - 1 + g_0)/Y$. Then Eq. (A2) can be represented in the form

$$z = \int_{\mu}^{\mu_1} \sqrt{\frac{c_0}{\alpha_0 \tilde{\kappa} \theta \sqrt{\theta^2 + 4\mu_b \theta + 1}}} d\theta = \int_{\mu}^{\mu_1} \sqrt{\frac{c_0}{\alpha_0 \tilde{\kappa}}} G(\theta) d\theta, \quad (\text{A8})$$

where we have introduced the notations

$$\mu = \frac{\hat{m}}{\sqrt{\tilde{\kappa}}}, \quad \mu_1 = \frac{\hat{m}_1}{\sqrt{\tilde{\kappa}_1}}, \quad \mu_b = \frac{\hat{m}_b}{\sqrt{\tilde{\kappa}}}, \quad \mu_{b1} = \frac{\hat{m}_b}{\sqrt{\tilde{\kappa}_1}}, \quad (\text{A9})$$

$$\hat{\kappa}_1 = \tau Y_1^{2/3} + 6\hat{m}_b^2, \quad Y_1 = 1 - g_0 + Y_1^{\epsilon/2} \left[\frac{\hat{\kappa}_1 + 6\hat{m}_1^2}{Gi} \right]^{-\epsilon/2}. \quad (\text{A10})$$

In order to estimate the integral in Eq. (A8) let's introduce an auxiliary function

$$\hat{G}(\theta) = -\ln \left[\frac{1 + 2\mu_b \theta + \sqrt{\theta^2 + 4\mu_b \theta + 1}}{\theta(1 + 2\mu_b)} \right], \quad (\text{A11})$$

and its differential

$$d \left[\frac{1}{\sqrt{\tilde{\kappa}}} \hat{G} \right] = \frac{d}{d\theta} \left[\frac{1}{\sqrt{\tilde{\kappa}}} \hat{G} \right] d\theta \\ = \frac{1}{\sqrt{\tilde{\kappa}}} \left(\frac{d\hat{G}}{d\theta} \right) d\theta - \frac{1}{2\tilde{\kappa}^{3/2}} \hat{G} \left(\frac{d\tilde{\kappa}}{d\theta} \right) d\theta. \quad (\text{A12})$$

Substituting the derivatives $(d\hat{G}/d\theta)$ and $(d\tilde{\kappa}/d\theta)$ in Eq. (A12) in its analytic expressions one obtains

$$d \left[\frac{1}{\sqrt{\tilde{\kappa}}} \hat{G} \right] = \frac{1}{\sqrt{\tilde{\kappa}}} G [1 + \epsilon(G_1 - G_2)] d\theta \\ = \frac{1}{\sqrt{\tilde{\kappa}}} G [1 + \mathcal{O}(\epsilon)] d\theta \approx \frac{1}{\sqrt{\tilde{\kappa}}} G(\theta) d\theta, \quad (\text{A13})$$

where

$$G_1 = \frac{4}{[1 - (\epsilon/2)Q]} \cdot \frac{(Y-1+g_0)}{Y} \cdot \frac{\mu_b}{(1+2\mu_b)} \cdot \frac{(1-w)}{(1+w)} \\ \cdot \frac{\tau Y^{2/3}}{\hat{\kappa}} \cdot \frac{\theta^2}{(1+6\theta^2)},$$

$$G_2 = \frac{3}{[1 - (\epsilon/2)Q]} \cdot \frac{(Y-1+g_0)}{Y} \\ \cdot \left(1 - \frac{2}{3} \frac{\tau Y^{2/3}}{\hat{\kappa}} \right) \ln \left[\frac{1 + 2\mu_b \theta + \sqrt{D}}{\theta(1 + 2\mu_b)} \right] \cdot \frac{\theta^2 \sqrt{D}}{(1+6\theta^2)},$$

$$w = \frac{\theta}{1 + \sqrt{D}}, \quad \sqrt{D} = \sqrt{\theta^2 + 4\mu_b \theta + 1}.$$

Using Eq. (A13) the integral at the right side of Eq. (A8) can be easily estimated, and the crossover expression for the order-parameter profile takes a form

$$z = \int_{\mu}^{\mu_1} \sqrt{\frac{c_0}{\alpha_0 \tilde{\kappa}}} G(\theta) d\theta \\ = \sqrt{\frac{c_0}{\alpha_0}} \int_{\mu}^{\mu_1} d \left[\frac{1}{\sqrt{\tilde{\kappa}}} \hat{G} \right] \\ = \sqrt{\frac{c_0}{\alpha_0 \tilde{\kappa}}} \ln \left[\frac{1 + 2\mu_b \mu + \sqrt{\mu^2 + 4\mu_b \mu + 1}}{\mu(1 + 2\mu_b)} \right] \\ - \sqrt{\frac{c_0}{\alpha_0 \tilde{\kappa}_1}} \ln \left[\frac{1 + 2\mu_{b1} \mu_1 + \sqrt{\mu_1^2 + 4\mu_{b1} \mu_1 + 1}}{\mu_1(1 + 2\mu_{b1})} \right]. \quad (\text{A14})$$

In the terms of the variables \hat{m} , \hat{m}_1 , \hat{m}_b , $\hat{\kappa}$, and $\hat{\kappa}_1$, Eq. (A14) reads

$$z = \bar{\xi}_0 \sqrt{\frac{Y}{\hat{\kappa}}} \ln \left[\frac{\hat{\kappa} + 2\hat{m}_b\hat{m} + \sqrt{\hat{\kappa}(\hat{m}^2 + 4\hat{m}_b\hat{m} + \hat{\kappa})}}{\hat{m}(\sqrt{\hat{\kappa}} + 2\hat{m}_b)} \right] - R_0, \tag{A15}$$

where the parameter

$$R_0 = \bar{\xi}_0 \sqrt{\frac{Y_1}{\hat{\kappa}_1}} \ln \left[\frac{\hat{\kappa}_1 + 2\hat{m}_b\hat{m}_1 + \sqrt{\hat{\kappa}_1(\hat{m}_1^2 + 4\hat{m}_b\hat{m}_1 + \hat{\kappa}_1)}}{\hat{m}_1(\sqrt{\hat{\kappa}_1} + 2\hat{m}_b)} \right], \tag{A16}$$

is analogous to the parameter z_0 in the MF approximation [see Eq. (14)].

The phenomenological generalization of the crossover expressions (A15) and (A16) obtained to the first order of ϵ can be obtained from Eq. (A1) with the replacements

$$a_R \rightarrow a_0 Y^{(1-\gamma)/\Delta}, \quad u_R \rightarrow u_0 Y^{(2\beta-\gamma)/\Delta}, \tag{A17}$$

$$c_0 \rightarrow c_R = c_0 Y^{(2\nu-\gamma)/\Delta}.$$

Formally reproducing the logic of the previous calculations, one can obtain in this case

$$z = \bar{\xi}_0 \frac{Y^{(\nu-\beta)/\Delta}}{\sqrt{\hat{\kappa}}} \ln \left[\frac{\hat{\kappa} + 2\hat{m}_b\hat{m} + \sqrt{\hat{\kappa}(\hat{m}^2 + 4\hat{m}_b\hat{m} + \hat{\kappa})}}{\hat{m}(\sqrt{\hat{\kappa}} + 2\hat{m}_b)} \right] - R_0, \tag{A18}$$

$$R_0 = \bar{\xi}_0 \frac{Y_1^{(\nu-\beta)/\Delta}}{\sqrt{\hat{\kappa}_1}} \times \ln \left[\frac{\hat{\kappa}_1 + 2\hat{m}_b\hat{m}_1 + \sqrt{\hat{\kappa}_1(\hat{m}_1^2 + 4\hat{m}_b\hat{m}_1 + \hat{\kappa}_1)}}{\hat{m}_1(\sqrt{\hat{\kappa}_1} + 2\hat{m}_b)} \right], \tag{A19}$$

$$Y = 1 - g_0 + Y^{(\gamma-2\beta)/\gamma} \left[\frac{1}{Gi} (\tau Y^{(1-2\beta)/\Delta} + \omega_1 \hat{m}^2 + \omega_2 \hat{m}_b^2) \right]^{-\Delta/\gamma}, \tag{A20}$$

$$Y_1 = 1 - g_0 + Y_1^{(\gamma-2\beta)/\gamma} \left[\frac{1}{Gi} (\tau Y_1^{(1-2\beta)/\Delta} + \omega_1 \hat{m}_1^2 + \omega_2 \hat{m}_b^2) \right]^{-\Delta/\gamma}, \tag{A21}$$

$$\hat{\kappa} = \tau Y^{(1-2\beta)/\Delta} + \omega_3 \hat{m}_b^2, \quad \hat{\kappa}_1 = \tau Y_1^{(1-2\beta)/\Delta} + \omega_3 \hat{m}_b^2, \tag{A22}$$

where ω_1 , ω_2 , and ω_3 are the universal constants.

APPENDIX B: CROSSOVER EXPRESSION FOR ADSORPTION

After the substitution of Eq. (50) in Eq. (18) and using the notations given in Eqs. (A3)–(A5) we have

$$\Gamma = \sqrt{\frac{c_0}{u_0}} \int_0^{\hat{m}_1} \frac{Y^{1/2} d\hat{m}}{\sqrt{\hat{m}^2 + 4\hat{m}_b\hat{m} + \hat{\kappa}}} = \sqrt{2\bar{m}_0} \bar{\xi}_0 \int_0^{\hat{m}_1} Y^{1/2} F(\hat{m}) d\hat{m}. \tag{B1}$$

In order to estimate the integral in Eq. (B1) we introduce an auxiliary function

$$\hat{F}(\hat{m}) = \ln \left[\left(\frac{Y_1}{Y} \right)^{1/3} \sqrt{\frac{\bar{\kappa}}{2\bar{m}_0^2 \hat{\kappa}_1}} \times (\hat{m} + 2\hat{m}_b + \sqrt{\hat{m}^2 + 4\hat{m}_b\hat{m} + \hat{\kappa}}) \right], \tag{B2}$$

and the differential

$$d[Y^{1/2} \hat{F}] = \frac{d}{d\hat{m}} [Y^{1/2} \hat{F}] d\hat{m} = Y^{1/2} \left(\frac{d\hat{F}}{d\hat{m}} \right) d\hat{m} + \frac{1}{2} Y^{-1/2} \hat{F} \left(\frac{dY}{d\hat{m}} \right) d\hat{m}, \tag{B3}$$

where in first ϵ -approximation $\bar{\kappa}$ and $\hat{\kappa}_1$ are given in Eqs. (12) and (A10). Replacing in Eq. (B3) the derivatives $(dY/d\hat{m})$ and $(d\hat{F}/d\hat{m})$ on their analytical expressions one can obtain

$$d[Y^{1/2} \hat{F}] = Y^{1/2} F [1 - \epsilon(F_1 + F_2 + F_3)] d\hat{m}, \tag{B4}$$

where the parameter Q is the same as in Eq. (A7), while the functions F_1 , F_2 , F_3 , and F are given by

$$F_1 = \frac{2}{[1 - (\epsilon/2) Q]} \cdot \frac{(Y - 1 + g_0)}{Y} \cdot \frac{\hat{m}}{(\hat{m} + 2\hat{m}_b + \sqrt{\hat{m}^2 + 4\hat{m}_b\hat{m} + \hat{\kappa}})} \cdot \frac{\tau Y^{2/3}}{(\hat{\kappa} + 6\hat{m}^2)}, \tag{B5}$$

$$F_2 = - \frac{2}{\left[1 - \frac{\epsilon}{2} Q\right]} \cdot \frac{(Y - 1 + g_0)}{Y} \cdot \frac{\hat{m} \sqrt{\hat{m}^2 + 4\hat{m}_b\hat{m} + \hat{\kappa}}}{(\hat{\kappa} + 6\hat{m}^2)}, \tag{B6}$$

$$F_3 = \frac{3}{[1 - (\epsilon/2) Q]} \cdot \frac{(Y - 1 + g_0)}{Y} \cdot \frac{\hat{m} \sqrt{\hat{m}^2 + 4\hat{m}_b\hat{m} + \hat{\kappa}}}{(\hat{\kappa} + 6\hat{m}^2)} \cdot \hat{F}(\hat{m}),$$

$$F = \frac{1}{\sqrt{\hat{m}^2 + 4\hat{m}_b\hat{m} + \hat{\kappa}}}. \tag{B7}$$

When $\hat{m}_1 \geq \hat{m} \geq 0$, the functions F_1 , F_2 , and F_3 have the final values ($\text{Const}_1 \geq F_1 + F_2 + F_3 \geq \text{Const}_2$), therefore, with an accuracy of the amplitude corrections of order of $\mathcal{O}(\epsilon)$ one can write

$$d[Y^{1/2} \hat{F}] = Y^{1/2} F [1 - \mathcal{O}(\epsilon)] d\hat{m} \approx Y^{1/2} F d\hat{m}. \tag{B8}$$

After substituting Eq. (B8) in Eq. (B1) and integrating

$$\Gamma = \Gamma_1 - \sqrt{2\bar{m}_0\bar{\xi}_0} Y_b^{1/2} \ln \left[\left(\frac{Y_1}{Y_b} \right)^{1/3} \sqrt{\frac{\bar{\kappa}}{2\bar{m}_0^2\hat{\kappa}_1}} (2\hat{m}_b + \sqrt{\hat{\kappa}_b}) \right], \quad (\text{B9})$$

where

$$\Gamma_1 = \sqrt{2\bar{m}_0\bar{\xi}_0} Y_1^{1/2} \ln \left[\sqrt{\frac{\bar{\kappa}}{2\bar{m}_0^2\hat{\kappa}_1}} \times (\hat{m}_1 + 2\hat{m}_b + \sqrt{\hat{m}_1^2 + 4\hat{m}_b\hat{m}_1 + \hat{\kappa}_1}) \right]. \quad (\text{B10})$$

The crossover function Y_1 to the first order of ϵ is defined in Eq. (A10) and Y_b is given by

$$Y_b = 1 - g_0 + Y_b^{\epsilon/2} \left[\frac{\hat{\kappa}_b}{Gi} \right]^{-\epsilon/2}, \quad (\text{B11})$$

where

$$\hat{\kappa}_b = \tau Y_b^{2/3} + 6\hat{m}_b^2. \quad (\text{B12})$$

In order to obtain the phenomenological generalization of the expressions (B9)–(B12) one should replace the coefficients a_R , u_R , and c_0 with their renormalized values as given by Eq. (A17). In this case the auxiliary function has the form

$$\hat{F}(\hat{m}) = \ln \left[\left(\frac{Y_1}{Y} \right)^{(1-2\beta)/2\Delta} \sqrt{\frac{\bar{\kappa}}{2\bar{m}_0^2\hat{\kappa}_1}} \times (\hat{m} + 2\hat{m}_b + \sqrt{\hat{m}^2 + 4\hat{m}_b\hat{m} + \hat{\kappa}}) \right], \quad (\text{B13})$$

where the crossover functions Y and Y_1 , and the parameters $\hat{\kappa}$ and $\hat{\kappa}_1$ are defined by Eqs. (A20)–(A22). Following the logic of the calculations used in the first ϵ -approximation we obtain

$$\Gamma = \sqrt{2\bar{m}_0\bar{\xi}_0} \int_0^{\hat{m}_1} Y^{(\nu-\beta)/\Delta} F(\hat{m}) d\hat{m} \quad (\text{B14})$$

$$= \Gamma_1 - \sqrt{2\bar{m}_0\bar{\xi}_0} Y_b^{(\nu-\beta)/\Delta} \ln \left[\left(\frac{Y_1}{Y_b} \right)^{(1-2\beta)/2\Delta} \times \sqrt{\frac{\bar{\kappa}}{2\bar{m}_0^2\hat{\kappa}_1}} (2\hat{m}_b + \sqrt{\hat{\kappa}_b}) \right], \quad (\text{B15})$$

where

$$\Gamma_1 = \sqrt{2\bar{m}_0\bar{\xi}_0} Y_1^{(\nu-\beta)/\Delta} \ln \left[\sqrt{\frac{\bar{\kappa}}{2\bar{m}_0^2\hat{\kappa}_1}} \times (\hat{m}_1 + 2\hat{m}_b + \sqrt{\hat{m}_1^2 + 4\hat{m}_b\hat{m}_1 + \hat{\kappa}_1}) \right], \quad (\text{B16})$$

and the crossover function Y_b along with the parameter $\hat{\kappa}_b$ are given by

$$Y_b = 1 - g_0 + Y_b^{\epsilon/2} \left[\frac{\hat{\kappa}_b}{Gi} \right]^{-\epsilon/2}, \quad \hat{\kappa}_b = \tau Y_b^{(1-2\beta)/\Delta} + \omega_3 \hat{m}_b^2. \quad (\text{B17})$$

- ¹A. Z. Patashinskii and V. L. Pokrovskii, *Fluctuation Theory of Phase Transitions*, 3rd ed. (Pergamon, New York, 1979).
- ²M. E. Fisher, in *Critical Phenomena, Vol. 186 of Lecture Notes in Physics*, edited by J. W. Hanhne (Springer-Verlag, Berlin, 1982), p. 1.
- ³M. E. Fisher and P.-G. de Gennes, *C. R. Acad. Sci., Paris B* **287**, 207 (1978).
- ⁴A. Clark, *The Theory of Adsorption and Catalysis* (Academic, New York, 1970).
- ⁵B. Rangarajan, C. T. Lira, and R. Subramanian, *AIChE. J.* **41**, 838 (1995).
- ⁶R. Subramanian, H. Pyada, and C. T. Lira, *Ind. Eng. Chem. Res.* **34**, 3830 (1995).
- ⁷R. Subramanian and C. T. Lira, in *Fundamentals of Adsorption*, edited by M. D. LeVan (Kluwer, Boston, 1996), pp. 873–880.
- ⁸C. A. Croxton, *Liquid State Physics-A Statistical Mechanical Introduction* (Cambridge University Press, London, 1974).
- ⁹D. Henderson, *Fundamentals Of Inhomogeneous Fluids* (Marcel Dekker, New York, 1992).
- ¹⁰J. F. Nicoll and P. C. Albright, *Phys. Rev. B* **31**, 4576 (1985).
- ¹¹C. Bagnuls and C. Bervillier, *Phys. Rev. B* **35**, 3585 (1987).
- ¹²M. Y. Belyakov and S. B. Kiselev, *Physica A* **190**, 75 (1992).
- ¹³M. A. Anisimov, S. B. Kiselev, J. V. Sengers, and S. Tang, *Physica A* **188**, 487 (1992).
- ¹⁴M. Y. Belyakov, S. B. Kiselev, and A. R. Muratov, *Sov. Phys. JETP* **77**, 279 (1993); **78**, 126 (1993).
- ¹⁵H. W. Diehl, *Int. J. Mod. Phys. B* **11**, 3503 (1997).
- ¹⁶L. Peliti and S. Leibler, *J. Phys. C* **16**, 2635 (1983).
- ¹⁷E. Brezin and S. Leibler, *Phys. Rev. B* **27**, 594 (1983).
- ¹⁸H. W. Diehl and M. Smock, *Phys. Rev. B* **47**, 5841 (1993); **48**, 6740 (1993).
- ¹⁹G. Floter and S. Dietrich, *Z. Phys. B: Condens. Matter* **97**, 213 (1995).
- ²⁰M. Y. Belyakov, S. B. Kiselev, and A. R. Muratov, *High Temp.* **33**, 701 (1995).
- ²¹S. B. Kiselev, L. Lue, and M. Y. Belyakov, *Phys. Lett. A* **251**, 218 (1999); **260**, 168 (1999).
- ²²J. R. Strubinger and J. F. Parcher, *Anal. Chem.* **61**, 951 (1989).
- ²³J. F. Parcher and J. R. Strubinger, *J. Chromatogr.* **479**, 251 (1989).
- ²⁴M. Thommes, G. H. Findenegg, and H. Lewandowski, *Ber. Bunsenges. Phys. Chem.* **98**, 477 (1994).
- ²⁵K. Binder, in *Phase Transition and Critical Phenomena*, edited by C. Domb and J. L. Lebowitz (Academic, London, 1983), Vol. 8.
- ²⁶H. W. Diehl, in *Phase Transition and Critical Phenomena*, edited by C. Domb and J. L. Lebowitz (Academic, London, 1986), Vol. 10, p. 76.
- ²⁷S. Dietrich, in *Phase Transition and Critical Phenomena*, edited by C. Domb and J. L. Lebowitz (Academic, London, 1988), Vol. 12, p. 1.
- ²⁸U. M. B. Marconi, *Phys. Rev. A* **38**, 6267 (1988).
- ²⁹t. C. Lubensky and M. H. Rubin, *Phys. Rev. B* **12**, 3885 (1975).
- ³⁰A. J. Bray and M. A. Moore, *J. Phys. A* **10**, 1927 (1977).
- ³¹L. D. Landau and E. M. Lifshitz, *Statistical Physics, Part. I*, 3rd ed. (Pergamon, New York, 1980).
- ³²J. Rudnick and D. Jasnow, *Phys. Rev. Lett.* **48**, 1059 (1982).
- ³³J. Rudnick and D. R. Nelson, *Phys. Rev. B* **13**, 2208 (1976).
- ³⁴M. Y. Belyakov, S. B. Kiselev, and J. C. Rainwater, *J. Chem. Phys.* **107**, 3085 (1997).
- ³⁵A. G. Liu and M. E. Fisher, *Phys. Rev. A* **40**, 2702 (1989).
- ³⁶J. H. Carpenter, B. M. Law, and D. S. P. Smith, *Phys. Rev. E* **59**, 5655 (1999).
- ³⁷S. B. Kiselev and V. D. Kulikov, *Int. J. Thermophys.* **18**, 1143 (1997).
- ³⁸S. B. Kiselev, *High Temp.* **24**, 375 (1986).
- ³⁹M. A. Anisimov and S. B. Kiselev, in *Sov. Tech. Rev. B. Therm. Phys.*, edited by A. E. Scheindlin and V. E. Fortov (Harwood, New York, 1992), Vol. 3, Part 2.
- ⁴⁰S. B. Kiselev and J. V. Sengers, *Int. J. Thermophys.* **14**, 1 (1993).
- ⁴¹S. B. Kiselev and J. C. Rainwater, *J. Chem. Phys.* **109**, 643 (1998).
- ⁴²J. F. Nicoll, *Phys. Rev. A* **24**, 2203 (1981).
- ⁴³J. Indekeu, *Phys. Rev. B* **36**, 7296 (1987).
- ⁴⁴M. Ley-Koo and M. S. Green, *Phys. Rev. A* **16**, 2483 (1977).

- ⁴⁵J. V. Sengers and J. M. H. Levelt Sengers, in *Progress in Liquid Physics*, edited by C. A. Croxton (Wiley, Chichester, U.K., 1978), p. 104.
- ⁴⁶M. E. Fisher (private communication).
- ⁴⁷P. J. Upton, Phys. Rev. Lett. **81**, 2300 (1998).
- ⁴⁸H. Frielinhaus, D. Schwahn, K. Mortensen, L. Willner, and K. Almdal, Physica B **234**, 260 (1997).
- ⁴⁹D. Schwahn, K. Mortensen, and S. Janssen, Phys. Rev. Lett. **73**, 1452 (1994).
- ⁵⁰D. Schwahn, T. Schmackers, and K. Mortensen, Phys. Rev. E **52**, 1288 (1995).
- ⁵¹D. Schwahn, S. Janssen, L. Willner, T. Schmackers, T. Springer, K. Mortensen, H. Takeno, H. Hasegawa, H. Jinnai, T. Hashimoto, and M. Imai, Physica B **213**, 685 (1995).
- ⁵²N. Kuwahara, H. Sato, and K. Kubota, Phys. Rev. Lett. **75**, 1534 (1995).
- ⁵³H. Seto, D. Schwahn, E. Yokoi, M. Nagao, S. Komura, M. Imai, and K. Mortensen, Physica B **213**, 591 (1995).